

Irregularities of ytterbium under high pressure

Y. C. Zhao,* F. Porsch, and W. B. Holzapfel

Fachbereich Physik, Universität-GH-Paderborn, D33095 Paderborn, Germany

(Received 30 August 1993)

Phase transitions of the rare-earth metal ytterbium were studied under pressure up to 70 GPa at room temperature with an energy-dispersive x-ray-diffraction technique using synchrotron radiation. A new phase transition $hcp \rightarrow fcc(II)$ was observed at 57 GPa. The phase sequence with pressure up to 70 GPa is $fcc(I) \rightarrow bcc \rightarrow hcp \rightarrow fcc(II)$. The hcp and $fcc(II)$ phases show some similarity in their compression behavior to the lower pressure phases of praseodymium which is considered as first evidence for a strong hybridization between f electrons and conduction electrons.

Ytterbium (Yb) is a member of the rare-earth metals or lanthanides (lanthanum though lutetium). However, it behaves irregular in comparison with other "regular" (trivalent) members of the lanthanide series due to its special electronic configuration. In solid state at ambient conditions, Yb is considered as divalent with an electronic configuration close to $4f^{14}(5d6s)^2$, whereas the other trivalent lanthanides are characterized by $4f^n(5d6s)^3$ with n going from 0 for lanthanum to 14 for lutetium. The special electronic configuration of Yb results first of all in a larger atomic volume at ambient condition and, furthermore, in a special sequence of phase transitions at ambient pressures and elevated temperatures as well as under pressure. In previous high-pressure studies¹⁻³ up to 39 GPa at ambient temperature, only the structural sequence $fcc \rightarrow bcc \rightarrow hcp$ was observed in contrast to $hcp \rightarrow Sm\text{-type} \rightarrow d\text{-hcp} \rightarrow fcc \rightarrow \text{distorted-fcc}$ for the regular (trivalent) lanthanides.^{4,5}

Theoretical considerations⁶ as well as x-ray absorption near-edge structure (XANES) experiments⁷ gave very strong indications for a change in the number of electrons per atom in the conduction band of Yb from almost 2 to almost 3 in the pressure range from 0 to 30 GPa, and theorists expected, therefore,^{8,9} that Yb under strong compression should ultimately follow also the structural sequence of the regular lanthanides. In this sense, the hcp phase could be considered as the first phase of the common structural sequence for all the regular trivalent lanthanides. Studies of the pressure-volume dependence by shock wave experiments^{10,11} resulted in an equation of state (EOS) for ambient temperature which was compatible with regular trivalent behavior above roughly 30 GPa; however, structural information could not be derived from these studies. The present study, therefore, gives the first information on the structural behavior in the higher-pressure range from 40 to 70 GPa at room temperature.

The present experiments were carried out with energy dispersive x-ray diffraction (EDXRD) using synchrotron radiation at HASYLAB, DESY (Hamburg). The details of this experimental station have been described previously.¹² High pressure was generated by a beveled diamond anvil cell¹³ (DAC) using an inconel gasket with a 100 μm hole. The collimator in front of the DAC was set to 60 μm . Silicone oil was used as pressure transmitting medi-

um which prevents also oxidation of the sample during sample loading. Fine ruby powder was loaded in the DAC as pressure sensor and the nonlinear ruby-luminescence scale¹⁴ was adopted for the pressure determination. The Yb sample material was provided by K. A. Gschneider, Jr., with chemical analysis giving the major impurity contents in atomic ppm as follows: 30 for iron, 30 for all other lanthanides, 304 for oxygen, and 1384 for hydrogen.

Figure 1 shows typical EDXRD pattern of Yb under pressure, where the lattice spacings d are related to the measured energies E by $Ed = 66.2528 \text{ keV \AA}$. The peak labeled G is from the gasket. The peak labeled X appears in all spectra with nearly constant relative intensity, and shifts with pressure less than other diffraction lines. Hence the peak X does not belong to pure Yb metal. The

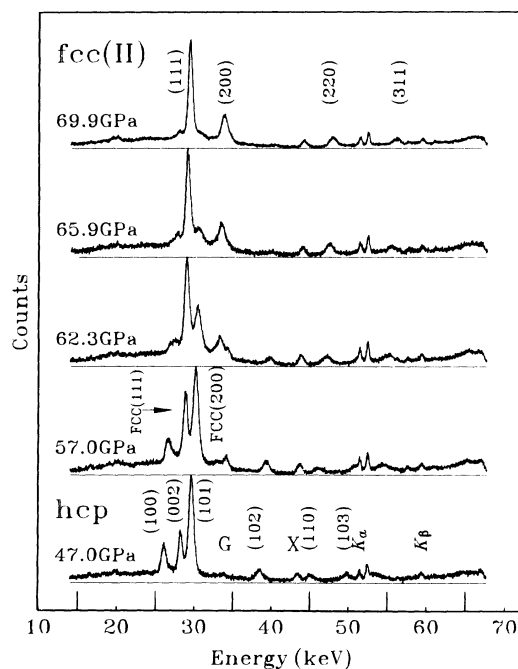


FIG. 1. Energy dispersive x-ray-diffraction spectra of Yb showing the evolution of the diffraction patterns for the $hcp \rightarrow fcc(II)$ transition under isothermal compression at room temperature.

lattice spacing of this peak varies from 0.1587 nm at 14.5 GPa to 0.1501 nm at 69.9 GPa and thus can neither be attributed to any diffraction line of YbO according to the volume-pressure relationship for the only presently known phase¹⁵ and hence remains unexplained. All structural changes below 39 GPa noticed in the present study are in agreement with the previous studies.¹⁻³ At higher pressures, however, a new phase transition hcp→fcc starts at about 57 GPa where the relative volume $V/V_0=0.40$, $a=0.287$ nm and $c=0.459$ nm for the hcp phase, and $a=0.403$ nm for the fcc phase, when the (111) and (200) lines of the new fcc phase appear. The difference of the atomic volume between these two phases is smaller than the experimental uncertainty ($<1\%$). With increasing pressure, the intensities for fcc lines (111), (200), (220), and (311) increase and the hcp lines disappear. In addition, the relative intensities of corresponding diffraction lines substantiate within the typical experimental limits this assignment of fcc structure. In order to distinguish between the two fcc phases below 4 GPa and above 57 GPa, the higher-pressure fcc phase is labeled fcc(II), while the low-pressure phase is labeled fcc(I). The reverse transition fcc(II)→hcp for decreasing pressure starts around 45 GPa, where $V/V_0=0.41$, $a=0.410$ nm for the fcc(II) phase, and almost finishes around 37 GPa. Thus, the present best estimate for the equilibrium transition pressure is 53(10) GPa and the atomic volume is $0.017(1)$ nm³.

Figure 2 shows the variation of atomic volume with pressure for Yb. Some previous EOS data for Yb from static measurements³ are also included in this figure to provide sufficient data for a smoothed representation of the EOS curve especially for the close-packed high-pressure phases hcp and fcc(II) together. Since theoretical consideration and experimental XANES studies on the electronic configuration of Yb under pressure gave strong evidence for the promotion of almost one complete f electron per atom to the conduction band in the pressure range from 0 to 30 GPa, it is useful to compare the present EOS data for the region above 30 GPa with the P - V variation for hypothetical "regular" trivalent Yb as it is given by the average of the EOS curves for Tm

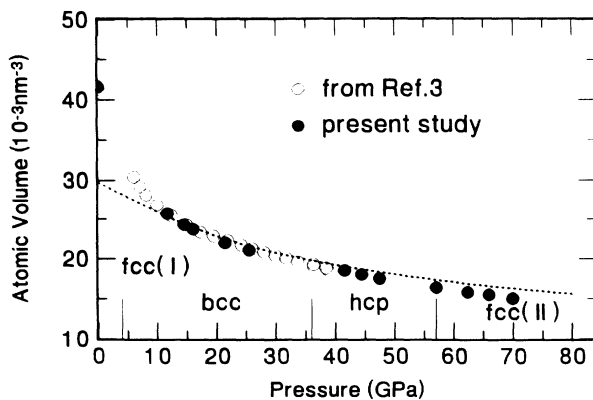


FIG. 2. Experimental isothermal pressure-volume data of Yb. Previous data (Ref. 3) are presented by open circles and the present data by solid circles. The dotted curve is the P - V variation of the hypothetical regular trivalent Yb.

and Lu, and represented by the dotted curve in Fig. 2. While the volume for hypothetical regular trivalent Yb is reached at about 15 GPa, further compression results, however, in a stronger volume decrease than expected for regular trivalent Yb or, in other words, Yb becomes softer than expected. A similar behavior is observed also for a few other trivalent lanthanides (Ce, Pr) and actinide elements (Am-Cf) when f electrons start to delocalize or start to contribute to bonding by strong hybridization with the conduction electrons.⁵

If one compares the structural sequence hcp→fcc(II) with the well-known sequence hcp→Sm-type→dhcp→fcc→distorted-fcc for the regular trivalent lanthanides, one can notice also that the intermediate structures Sm-type and dhcp are missed. Hence the phase transition hcp→fcc(II) does not fit to the behavior of the regular lanthanides. In addition, the measured c/a values for the hcp phase in Yb is 1.60 in contrast to 1.57–1.59 of hcp phases in the trivalent lanthanides, and thus are closer to the ideal c/a value (1.633) of the hcp lattice than in the regular trivalent lanthanides.

Furthermore, the common sequence of phase transitions in the regular trivalent lanthanides can be characterized by radius ratios^{5,16} R_{WS}/R_{5p} , where R_{WS} is the Wigner-Seitz radius and R_{5p} represents the radius of the $5p$ electron orbital of trivalent ion of lanthanide given in Ref. 17. At the equilibrium transition pressure for the hcp→fcc(II) transition in Yb (at 53 GPa), $R_{WS}=0.159$ nm and thus $R_{WS}/R_{5p}=2.48$, whereas the common value of R_{WS}/R_{5p} that characterizes the dhcp→"fcc" transition of the regular trivalent lanthanides^{5,16} is 2.46(4). Thereby "fcc" stands for either the fcc structure or the distorted-fcc structure which is directly formed from dhcp at room temperature in the case of the heavier lanthanides (Tb-Lu). Thus, a comparison of the R_{WS}/R_{5p} value for the hcp→fcc(II) transition of Yb with that for the regular lanthanides at the dhcp→"fcc" transition shows that the difference is within the typical scatter of these values for the other (heavier) lanthanides; however, the appearance of the superlattice diffraction lines for this distorted-fcc phase of regular trivalent lanthanides is not observed.

Finally one can evaluate the EOS data for the two close-packed high-pressure phases hcp and fcc(II) together in the scaling scheme extensively used in a recent comparison of EOS data for regular and irregular lanthanides with actinides under pressure.^{18,19} Thereby the pressure P was scaled by the pressure of the corresponding Fermi gas pressure $P_{FG}=a_{FG}(Z/V)^{5/3}$ where $a_{FG}=23.37$ MPa nm⁵, Z is the atomic number, and V stands for the atomic volume represented by the volume of the Wigner-Seitz cell. If one uses in addition the scaled atomic radius $\sigma=[3ZV/(4\pi)]^{1/3}$ with its value σ_0 at ambient condition, one can represent the EOS data in a scaled form by a plot of the quantity $\eta=\ln(P/P_{FG})-\ln(1-\sigma/\sigma_0)$ versus σ as shown in Fig. 3, which allows for direct comparison of EOS data for different elements and especially within the lanthanide and actinide families as discussed in detail previously.¹⁸⁻²⁰ More specifically, the EOS data of all the regular trivalent lanthanides are presented in this scaled form within the given experimental error just

by a common relation, which is represented in Fig. 3 by the slightly curved dashed line and starts at the common value $\sigma_0=0.792(3)$ nm for all the regular trivalent lanthanides.¹⁵ Besides the irregular lanthanides (Ce, Eu, and Yb) also the elements La and Pr show already at rather low pressures (<20 GPa) significant deviations from this common behavior as illustrated by the dash-dotted line just for Pr in Fig. 3. The data for the bcc phase of Yb already discussed in Ref. 18 are represented here again by the open circles.

Since the values of η in this representation depend on the value for σ_0 used in the scaling, one must be careful with the interpretation of data for high-pressure phases like the data for Yb in the hcp and fcc(II) phases represented in Fig. 3 by open diamonds and squares, which correspond to the use of $\sigma_0=0.883$ nm for the low-pressure (divalent) fcc(I) phase. For a comparison with the regular trivalent behavior, the use of the common trivalent value for $\sigma_0=0.792(3)$ nm is more appropriate for these high-pressure phases, corresponding to an extrapolation of the EOS for the hypothetical regular trivalent Yb to ambient condition. Scaled with this σ_0 value, the EOS data of the close-packed high-pressure phases of Yb (indicated by solid diamonds and squares in Fig. 3) show some similarity to the irregular behavior of Pr before its volume collapse transition. On the basis of the EOS behavior of Yb one is therefore also led to the conclusion, that Yb in these close-packed high-pressure phases does not show typical behavior of a simple or regular trivalent lanthanide metal, but is effected like Pr in its low-pressure phases already by significant contributions of hybridization between the still almost localized *f* electrons with the conduction electrons, in other words, by weak *f* electron bonding.

Note added in proof. Our latest measurements on Yb up to 90 GPa confirm that the peak marked with X results not from the Yb sample since it does not occur in

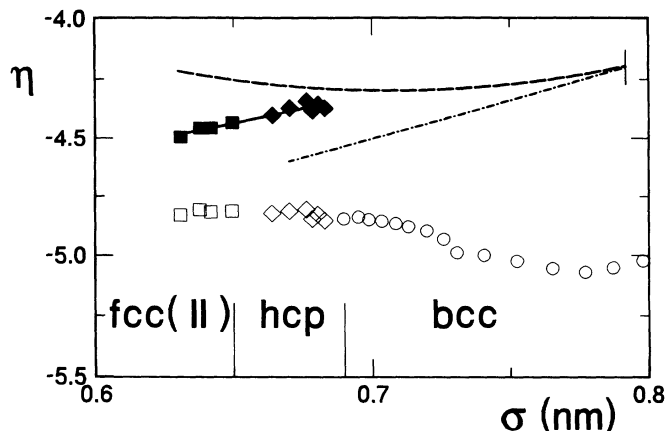


FIG. 3. Compression data of Yb in η - σ representation with $\eta = \ln(P/P_{FG}) - \ln(1 - \sigma/\sigma_0)$. The experimental compression data for hcp and fcc(II) scaled with the value of $\sigma_0=0.792(3)$ nm for the regular trivalent lanthanides are indicated by solid diamonds and squares, respectively. The data for hcp and fcc(II) scaled with the divalent value of $\sigma_0=0.883$ nm are indicated by the open diamonds and squares. The dashed curve indicates the EOS for the hypothetical regular trivalent Yb and the dash-dotted line the compression behavior of Pr before its volume-collapse transition. The data for the bcc phase taken from literature^{3,18} are shown by open circles.

these new measurements, and the stability of the phase fcc(II) extends up to 90 GPa.

This work is supported in parts by the Deutsche Forschungsgemeinschaft, the Bundesministerium für Forschung und Technologie and HASYLAB, DESY. The authors would like to thank Professor K. A. Gschneider, Jr. for providing the sample material and W. Sievers, O. Schulte, M. Winzenick, and J. Otto for assistance in the experiment. One of the authors (Y.C.Z.) is indebted to Alexander von Humboldt-Stiftung for financial support.

*Permanent address: Beijing Synchrotron Radiation Facility, P.O. Box 918, 2-7, Beijing 10039, People's Republic of China.

¹W. B. Holzapfel, T. G. Ramesh, and K. Syassen, *J. Phys. (Paris) Colloq.* **40**, C5-390 (1979).

²K. Takemura and K. Syassen, *J. Phys. F* **15**, 543 (1985).

³W. A. Grosshans, Ph.D. thesis, University of Paderborn, 1987.

⁴A. Jayaraman, *Phys. Rev. A* **135**, 1056 (1964), D. B. McWhan, *Science* **176**, 751 (1972); K. A. Gschneider, Jr. and F. W. Calderwood, in *Handbook on the Physics and Chemistry of Rare Earths*, edited by K. A. Gschneider, Jr. and L. Eyring (Elsevier, New York, 1986), Vol. 8, p. 1.

⁵U. Benedict, W. A. Grosshans, and W. B. Holzapfel, *Physica* **144B**, 14 (1986) and references therein.

⁶J. F. Herbst and J. W. Wilkins, in *Handbook on the Physics and Chemistry of Rare Earths*, edited by K. A. Gschneider, Jr., L. Eyring and S. Hufner (Elsevier, New York, 1987), Vol. 10, p. 321.

⁷K. Syassen, G. Wortmann, J. Feldhaus, K. H. Frank, and G. Kaindl, *Phys. Rev. B* **26**, 4745 (1982).

⁸B. Johansson and A. Rosengren, *Phys. Rev. B* **11**, 2836 (1975).

⁹H. L. Skriver, *Phys. Rev. Lett.* **49**, 1768 (1982); *Phys. Rev. B* **31**, 1909 (1985).

¹⁰W. H. Gust and E. B. Royce, *Phys. Rev. B* **8**, 3595 (1973).

¹¹W. J. Carter, J. N. Fritz, S. P. Marsh, and R. G. McQueen, *J. Phys. Chem. Solids* **36**, 741 (1975).

¹²For example, W. A. Grosshans, E.-F. Düsing, and W. B. Holzapfel, *High Temp. High Pressure* **16**, 539 (1984).

¹³K. Syassen and W. B. Holzapfel, *Europhys. Conf. Abstr.* **1A** 75 (1975); W. B. Holzapfel, in *High Pressure Chemistry*, edited by H. Kelm (Reidel, Boston, 1978), p. 177.

¹⁴H. K. Mao, P. M. Bell, J. W. Shaner, and D. J. Steinberg, *J. Appl. Phys.* **49**, 3276 (1978).

¹⁵A. Werner, H. D. Hochheimer, A. Jayaraman, and J. M. Leger, *Solid State Commun.* **38**, 325 (1981).

¹⁶T. Krüger, B. Merkau, W. A. Grosshans, and W. B. Holzapfel, *High Pressure Res.* **2**, 193 (1990).

¹⁷J. T. Waber and D. T. Crommer, *J. Chem. Phys.* **42**, 4116 (1965).

¹⁸W. A. Grosshans and W. B. Holzapfel, *Phys. Rev. B* **45**, 5171 (1992).

¹⁹W. B. Holzapfel, *Physica* **B190**, 21 (1993), and references therein.

²⁰W. B. Holzapfel, *Europhys. Lett.* **16**, 67 (1991); in *Molecular Solids Under Pressure*, edited by R. Pucci and G. Piccitto (North-Holland, Amsterdam, 1991), p. 61.